# Evaluating Model-Estimated Shoulder Muscle Activity During Overhead Work with Varied Task Demands and Exoskeleton Use

Lingyu Li

Thesis submitted to the faculty of the Virginia Polytechnic Institute and State University in partial fulfillment of the requirements for the degree of

Master of Science
In
Industrial and Systems Engineering

Maury A. Nussbaum, Chair
Michael L. Madigan
Sunwook Kim

May 9th, 2025
Blacksburg, Virginia

Keywords: Exoskeleton Modeling, Musculoskeletal Modeling, Shoulder WMSD

# Evaluating Model-Estimated Shoulder Muscle Activity During Overhead Work with Varied Task Demands and Exoskeleton Use

Lingyu Li

## ABSTRACT

Passive arm-support exoskeletons (ASEs) have emerged as an intervention that can reduce shoulder stress during overhead tasks. However, the effects of these devices are task- and device-specific, and current evaluation protocols remain time-consuming and resource-intensive. Musculoskeletal modeling could simplify the process of ASE evaluation, by replacing electromyography (EMG) sensors with estimates of muscle activation. However, there is no existing evidence to determine whether model performance with ASE is sufficient or consistent under varied task demands. In this study, I evaluated estimates of shoulder muscle activity generated by one commercial biomechanical model, during dynamic overhead push tasks at different heights and directions, both with and without an ASE. Kinematics and external load data were input into the AnyBody Modeling System to simulate muscle activation. Model estimates were then compared to normalized EMG using pattern similarity and magnitude difference metrics. Overall, the results obtained demonstrated good model performance with relatively smaller arm elevation, but that model performance decreased as arm elevation increased and that ASE use further impaired model performance. These findings indicate that model-estimated shoulder muscle activity is reasonably accurate under specific task conditions. However, improvements to musculoskeletal models are necessary to make these models suitable for a broader range of tasks.

Evaluating Model-Estimated Shoulder Muscle Activity During Overhead Work with Varied Task Demands and Exoskeleton Use

Lingyu Li

## GENERAL AUDIENCE ABSTRACT

Passive arm support exoskeletons (ASEs) are wearable devices designed to reduce shoulder strain during overhead work. However, their effectiveness varies with the type of task, and testing these devices requires expensive and time-consuming measurements of muscle activity (among other outcomes). Computer simulations could replace some of these measurements, especially muscle activity, but the accuracy of such simulations during complex tasks when an ASE is used has not been evaluated. In this study, I used recorded body movements and hand push forces when participants performed overhead push tasks at different heights and directions, both with and without an ASE. These data were input into a commercial computer model of the shoulder, and model-estimated muscle activity was compared to actual readings (via electromyography). I quantified model performance both in terms of how closely the patterns of predicted and measured activity matched and by how much the magnitudes of these activities differed. The model performed well at low heights, with relatively smaller arm elevation, but model predictions became less accurate as the arm was raised higher. Model accuracy was also lower when using it to simulate tasks with an ASE. These findings suggest that computer models can make reasonable predictions of shoulder muscle activity for certain task conditions. However, the models require further improvement before replacing physical measurements across a wider range of tasks.

Table of Contents

## 1. Introduction

Work-related musculoskeletal disorders (WMSDs) are conditions common in the working environment that affect nerves, tendons, muscles, and supporting structures of the human body. (Bernard & Putz-Anderson, 1997). WMSDs remain an important health problem worldwide. In the European Union, for example, roughly 60% of workers reported complaints about WMSDs in 2015, and over 40% reported cases related to the shoulder, neck, and upper limbs (de Kok et al., 2019). In the United States, upper extremity WMSDs (UE-WMSDs) remain one of the most common types, contributing to nearly a third of almost 250,000 recorded days-away-from-work cases in 2020 (U.S. Bureau of Labor Statistics, 2020). Shoulder WMSDs in particular contributed to about half of all UE-WMSD cases in 2020, with a median of 25 days away from work (U.S. Bureau of Labor Statistics, 2020). Therefore, approaches to reduce UE-WMSD risk are clearly needed to enhance workplace safety and reduce costs due to lost productivity and medical expenses.

Most such approaches are designed to reduce exposure to WMSD risk factors. Risk factors for shoulder WMSDs include forceful exertion, repetitiveness, and non-neutral arm postures (e.g., Roquelaure et al., 2009; Alwasel et al., 2011). Overhead work, a well-established risk factor (e.g., Sommerich & Hughes, 2006; Van der Molen et al., 2017; Wærsted et al., 2020), is prevalent but difficult to avoid in some occupational settings. For instance, automotive assembly lines often require overhead assembly tasks, and construction tasks involving drywall, plumbing, or HVAC commonly require overhead work. While various ergonomics controls can mitigate exposure to shoulder WMSD risk factors, these controls are often impractical or infeasible. For example, Albers and Estill (2007) suggested raising and placing building materials with hoists

and using lifts to raise workers to reduce overhead reaching distance. However, equipment costs or site conditions could restrict the implementation of such approaches. Additional solutions to mitigate WMSD risk factors are necessary, especially when these risk factors are difficult to avoid.

Exoskeletons (EXOs) are "wearable devices that augment, enable, assist, and/or enhance physical activity through mechanical interaction with the body" (Lowe et al., 2019). EXOs follow a user's movements, providing mechanical support while retaining the flexibility and creativity of human workers (de Looze et al., 2016). These properties enable EXOs to mitigate exposures to WMSD risk factors while minimizing modifications to working environments. We can categorize EXOs based on the supported body parts, with the most common types at present being arm-support exoskeletons (ASEs) or back-support exoskeletons (BSEs). We can also categorize EXOs by the power source, as passive or active. Passive EXOs generate torques or forces due to the deformation of compliant parts, such as elastic material or springs. In contrast, active EXOs include powered torque or force-generating mechanisms, such as motors, and external power sources (usually from batteries). This thesis focused on passive ASEs due to their more extensive commercial availability and given that active devices are mostly still in development or research stages. Moreover, passive devices are less costly and easier to implement, suggesting their substantial near-term potential for mitigating UE-WMSD risk factors in occupational activities.

Existing lab-based studies have demonstrated the efficacy of passive ASEs in reducing muscle activity during simulated occupational tasks, showing reductions of shoulder muscle activity by up to ~50%. (De Bock et al., 2021; Desbrosses et al., 2021; Grazi et al., 2020; Kim et al., 2018;

Pacifico et al., 2022; Rashedi et al., 2014; Zhou & Zheng, 2021). However, these studies have also clearly shown that the effect of an EXO is task-and-EXO-specific, and that EXO use for some tasks could result in no or adverse effects on task performance (Gillette & Stephenson, 2019; Kim et al., 2021; Ojelade et al., 2023). Therefore, assessing the effects of ASEs for specific tasks is necessary to implement these devices effectively, but performing human-subject studies for such assessment is time-consuming and resource-intensive. Simplifying assessment processes would enhance occupational EXO implementations.

A central assumption of this thesis is that human-exoskeleton models could simplify the process of identifying suitable ASE use cases. These models combine human musculoskeletal models and virtual EXOs, incorporating properties of both the human musculoskeletal system and EXOs. With body kinematics and external forces as inputs, human-exoskeleton models can generate various biomechanics measurements, such as muscle activity, joint reaction force, and energy consumption. If such estimations are accurate, identifying suitable ASE use cases would be less time-consuming. For instance, monitoring muscle activity often involves using EMG sensors. These sensors are expensive, and the setup process is time-consuming. Model-estimated muscle activities could replace EMG sensors if such estimations are accurate.

Existing work has used human-exoskeleton models to simulate the effects of EXOs. These models benefit both the early design and final implementation stages of EXOs (Auer et al., 2022). During the early design stage of EXOs, designers have used human-exoskeleton models to simulate the potential benefits and side effects of EXO prototypes (Blanco et al., 2019; Troster et al., 2020) or to compare different EXO prototype designs (Gneiting et al., 2022). For the final implementation stage of commercial exoskeletons, Schmalz et al. (2022) and Madinei and

Nussbaum (2023) estimated spine loads during lifting tasks with and without a BSE. Seiferheld et al. (2022) used a human-exoskeleton model to estimate shoulder muscle activity and joint reaction force for an in-field ASE test. Fritzsche et al. (2021) compared estimated and measured anterior deltoid muscle activities during an overhead drilling task, and they found a close match between the two. Similarly, Kong et al. (2022) reported agreement between measured and estimated leg muscle activity when performing occupational tasks with a lower limb exoskeleton.

Though finding agreements between estimated and estimated muscle activity, these latter two studies were limited to fairly simple tasks (Kong et al., 2022) or only compared muscle activities from two muscle group (Fritzsche et al., 2021). Due to limited EMG data and task variations, the accuracy of estimated muscle activity for other shoulder muscle groups or under different task conditions remains unclear. Aurbach et al. (2020) reported a discrepancy between estimated and measured deltoid muscle activity patterns when the shoulder abduction angle exceeded 90°, with a more pronounced mismatch in the lateral and posterior deltoid. This finding aligns with Nikooyan et al. (2010) and Nikooyan et al. (2011), who also observed mismatches between model-estimated muscle activity or joint reaction forces and in vivo measurements at elevated arm postures. Moreover, to my knowledge, no existing evidence indicates whether musculoskeletal models perform differently when an ASE is included.

Therefore, my thesis focused on examining how ASE use influences model-estimated shoulder muscle activity and whether task conditions affect these estimations. I compared model-estimated shoulder muscle activity with normalized EMG during overhead tasks that require hand exertion at three heights and two directions, with and without an ASE. I derived pattern

similarities and magnitude differences as metrics to compare measured and estimated shoulder muscle activity. My first hypothesis was that the model-estimated shoulder muscle activity would correlate well with NEMG at lower task heights under both ASE and the control condition. My second hypothesis was that ASE use would adversely affect these metrics, particularly at higher task heights. These hypotheses were based on the fact that the ASE model used here was relatively simple and thus may not capture changes in contact points caused by relative movement between the ASE and the human body. Such relative motion becomes more pronounced at elevated arm postures. Given that shoulder musculoskeletal model performance reduces at higher arm elevations without ASE use, I expected this reduction to be exacerbated with ASE use.

## 2. Methods

### 2.1 Experimental Setup

I used a subset of data from a previous study conducted in the Occupational Ergonomics and Biomechanics (OEB) laboratories at Virginia Tech. That study was designed to assess the efficacy of three ASEs during simulated overhead tasks. A total of 18 gender-balanced participants were recruited from Virginia Tech and local communities. No participant self-reported musculoskeletal disorders or injuries in the past 12 months.

Participants performed dynamic overhead push tasks representing typical motions during the final automotive assembly. These tasks included three heights and two push directions, and participants completed these tasks with three ASEs and without any ASE. I included one ASE in the current work, specifically the shoulderX (V3, SuitX, Emeryville, United States), because the manufacturer provided us with a detailed CAD assembly and torque profile of this Device. This

assembly provided the necessary mechanical properties of shoulderX for modeling purposes, such as dimensions and joint connections.

The task design of this previous study created diverse demands on the shoulder muscles by creating different overhead working scenarios, thereby helping to identify potential limitations of our models. Results from Ojelade et al. (2023) and Chopp et al. (2010) indicate that push directions and task heights significantly affect shoulder muscle activity, while Chopp et al. (2010) further showed that shoulder flexion angles in overhead tasks also influence muscle activity. Therefore, including several combinations of heights and push directions will result in a range of shoulder muscle activity levels.

The previous study specified task heights with the same approaches from Ojelade et al. (2023). This method defined two reference heights: hand height when the shoulder flexes 60° and the forearm upright (A) and hand height when the arm is fully flexed with the shoulders in a neutral position (maximum overhead reach with no shoulder elevation, B). Low, medium, and high heights were defined based on these reference measures as A, A + 0.53(B – A), and A + 0.7(B – A), respectively. As in the study by Ojelade et al. (2023), two triaxial loadcells (AMTIMCA3a-6, Watertown, MA, USA) were attached to a height-adjustable workpiece, one facing downward and one toward the participant. This allowed for measuring forces during two corresponding push directions, specifically upward and forward. The combinations of work heights and push directions resulted in six task conditions (Figure 1).

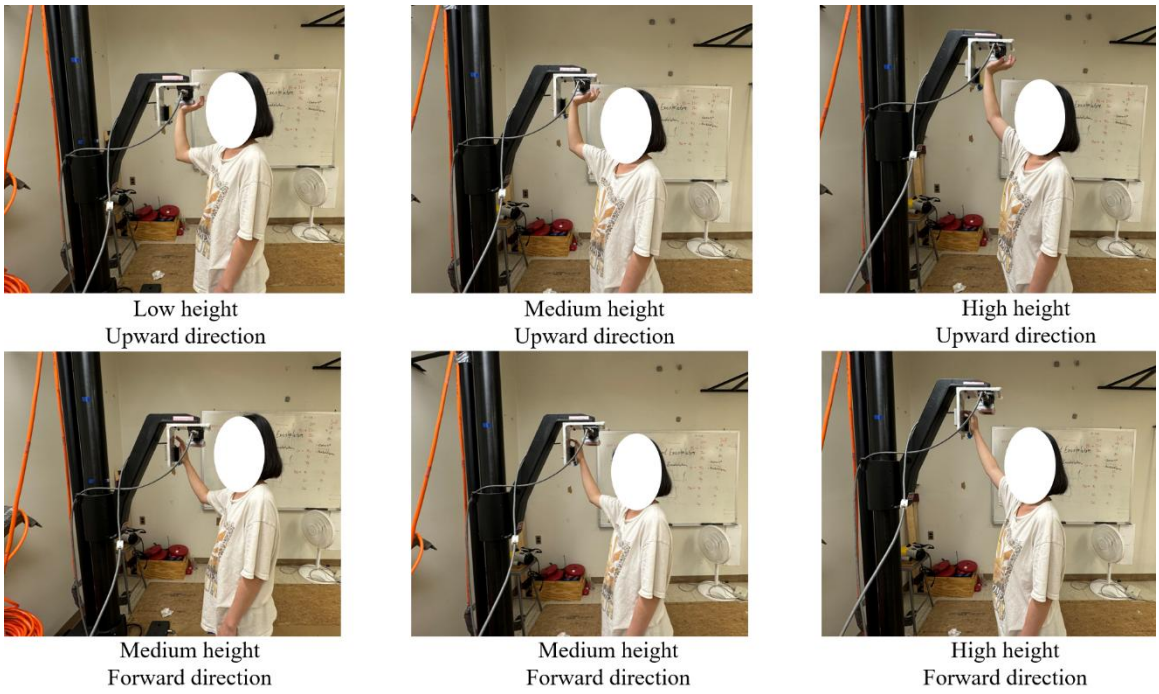


Figure 1. Illustration of six simulated task conditions (three work heights and two push directions).

To complete each task, participants pushed a load cell 10 times per minute, following a digital metronome. For each push, participants needed to exert normal forces above 53N when pushing forward and 75N when pushing upward. An audio tone provided feedback whenever the exerted force exceeded these thresholds. The thresholds and exertion rate were designed to reflect the demands of automotive manufacturing based on input from subject matter experts. The presentation order of interventions (three ASE conditions and one control condition with no ASE) was counterbalanced using multiple 4 × 4 Latin Squares. Under each intervention, the work height was counterbalanced with 3 × 3 Latin Squares, and the order of push directions was altered across participants. In this thesis, I analyzed data with all combinations of work height and push directions under two interventions (shoulderX and control). To reduce fatigue, participants rested for at least two minutes between tasks.

Muscle activity was recorded (at 1500 Hz) with a wireless EMG system (Noraxon Ultium EMG, Noraxon, Scottsdale, AZ). After proper skin preparation, investigators placed electrodes (Ag/AgCl, with a 2.5 cm inter-electrode spacing) unilaterally on the dominant side of the participant to record muscle activity from the deltoid (anterior, middle, and posterior portions), upper trapezius, serratus anterior, pectoralis major and infraspinatus. Activity of the sternocleidomastoid and erector spinae was recorded bilaterally.

Before completing the pushing trials, participants performed maximum voluntary isometric contractions (MVICs). For the shoulder muscle groups, participants flexed their arms at 60° and raised their arms with maximum strength at horizontal abduction angles of 60°, 90°, and 120°. During these MVICs, participants held a handle anchored to the floor with a chain while investigators applied manual resistance to the participants' arms. For each MVIC, investigators ensured the correct postures of participants and instructed participants to gradually increase the force to their maximum, hold at maximum for three seconds, and gradually decrease the force. Investigators also provided non-threatening verbal encouragement during each MVIC. Participants performed each MVIC twice, with at least 60 seconds of rest between each MVIC.

Investigators captured full-body kinematics with a markerless motion capture (MMC) system (Azure Kinect, Microsoft Corporation, Seattle, WA, USA) at 15 Hz. Two cameras were placed orthogonally about 2.5 m from the participant. Results from the pilot work showed that this arrangement can effectively capture the 3D motion of the right arm during the overhead pushing tasks.

## 2.2 Data Pre-processing

I filtered the MVIC and overhead task EMG data with a bidirectional, 4th-order Butterworth bandpass filter (25-450 Hz) to remove low- and high-frequency noise, followed by a 300 ms root-mean-square moving window to extract linear envelopes. I then normalized the EMG data by dividing each data point by the maximum muscle activity obtained from the MVICs. I extracted Biovision Hierarchy (BVH) data from the MMC system recordings and filtered the BVH files with a low-pass filter (5 Hz, 4th-order Butterworth, bidirectional) to remove noise and artifacts.

### 2.3 Human-exoskeleton Model

I built a human-exoskeleton model with a commercial biomechanical modeling platform, the AnyBody Modeling System (AMS: version 8.0, AnyBody Technology, Aalborg, Denmark). I used the AnyBody managed modeling Repository (AMMR) v3.0.1. The shoulder of this musculoskeletal model is based on a model by Van Der Helm (1994). It includes a detailed shoulder complex, with the shoulder girdle movement determined by the glenohumeral joint angle.

Earlier studies have evaluated this model in several ways. Nikooyan et al. (2010) compared estimated glenohumeral joint reaction forces (GH-JRF) with *in vivo* measurements. During arm flexion and abduction up to 90°, the estimated GH-JRF and *in vivo* measurement had Pearson correlation coefficients (R) above 0.96 for the two participants in their study. However, the estimated GH-JRF started to decrease above 90° arm elevation angle, whereas *in vivo* GH-JRF kept increasing. Additionally, during static force exertion, this model overestimated peak GH-JRF. Nikooyan et al. (2011) compared model-estimated muscle force with EMG measurements, finding that most estimated muscle forces from three optimization methods followed the pattern

of EMG signals (mean $R > 0.6$ across all muscles). However, some estimated antagonist muscle forces during shoulder flexion were inconsistent with EMG signals. Based on the evidence above, the shoulder model in AMS can estimate muscle force and GH-JRF with reasonable accuracy in several scenarios. Therefore, I decided to use this model as a base to build a shoulder human-exoskeleton model.

I included a virtual shoulderX in AMS to create a human-exoskeleton model. The shoulderX was designed to support the shoulder against gravitational force and external load during elevated shoulder postures (Van Engelhoven et al., 2018a). A user can independently adjust the torque profile for each arm to suit different working conditions. This Device is adjustable in hip width and depth, torso length, shoulder width, and arm length to fit wearers of different body sizes. Previous research has examined the shoulderX in both simulated tasks (De Bock et al., 2021; Ojelade et al., 2023; Pinho & Forner-Cordero, 2022; Pinho et al., 2020; Van Engelhoven et al., 2018a) and during field testing (De Bock et al., 2021). These studies showed that shoulderX could reduce shoulder muscle activity during overhead tasks, but that muscle activity reductions could be less substantial during field vs. lab-based testing. The isolated overhead tasks in this study are consistent with the expected use conditions of the shoulderX.

The shoulderX consists of five main components: one torso frame, two shoulder frames, and two arm frames (Figure 2). For the simplicity of my model, I only included the right shoulder and arm frames of the shoulderX, as the overhead exertions involved the dominant hand, and all participants were right-handed. In reality, the torso frame attaches to the wearer's torso with a belt and backpack straps, allowing slight movement between the torso frame and the body. The shoulder frame connects to the torso frame via a rotational joint located above the acromion.

Therefore, the shoulder frame in my model was connected to a point above the acromion via a rotational joint, with the joint constraint defined as soft to allow slight movement between the shoulder frame and the defined point. The shoulder frame connects to the arm frame with a rotational joint that generates torque when support is turned on. The arm frame connects to the upper arm with a pad and strip. This structure allows the upper arm to rotate and slide relative to the arm frame, so I allowed these relative movements between the arm frame and the humerus in my model.


Figure 2. Segments of the shoulderX

Support torque is generated at the joints connecting the arm frames to the shoulder frames. I incorporated this torque as a function of arm elevation angle, based on the torque profile provided by the manufacturer. The support torque is transmitted to the upper arm as a contact force applied at a fixed contact point (Figure 3) along the humeral. The distance of this contact point from the glenohumeral joint was determined using each participant's anthropometric data, since the arm frame length is adjustable to fit users of different sizes.

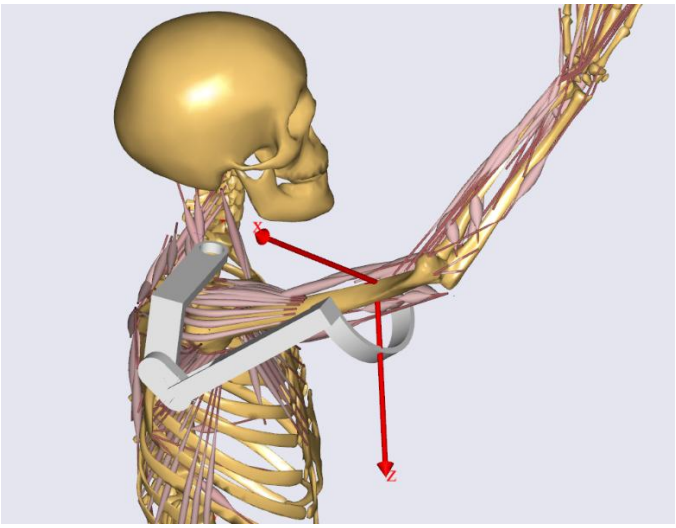

Figure 3. Illustration of the location of shoulderX and upper arm contact point

2.4 Model Simulations

I input kinematics and loadcell data into AMS to perform inverse dynamic analysis. The human musculoskeletal system contains more muscles than joint degrees of freedom, and usually, muscles collaborate to perform movements. Such features make the human musculoskeletal system statically indeterminate, and there exist infinitely many combinations of muscle forces that can achieve mechanical equilibrium. Musculoskeletal modeling platforms typically solve optimization problems to simulate muscle forces, using:

$$\text{minimize } G(f)$$

$$\text{subject to } Cf = r$$

where $G$ represents an objective function, $C$ represents a matrix of coefficients, $f$ represents an array of muscle forces, and $r$ represents resultant joint forces and moments.

Different muscle recruitment criteria have been developed to simulate muscle recruitment, and a major difference between these criteria is the objective function, $G$. I used two criteria as objective functions. One criterion is polynomial, which minimizes the summation of muscle stress raised to a power $p$ (Crowninshield & Brand, 1981; Michaud et al., 2021):

$$polynomial\colon\ G = \sum_i \left(\frac{f_i}{N_i}\right)^p$$

where $N_i$ are normalization factors (e.g., muscle strength). Crowninshield and Brand (1981) found that power between 1.4 and 5.1 minimizes muscle fatigue, and the mean value across experiments was 3.0. Another criterion is minmax, which minimizes the maximum relative muscle force (Rasmussen et al., 2001):

$$minmax\colon\ G = \max\left(\frac{f_i}{N_i}\right), i = 1, 2, \dots, n$$

Both criteria are physiologically reasonable, as they distribute forces across muscles and minimize muscle stress or fatigue. I simulated muscle activity using minmax, polynomial with a power $p$ of 2, and polynomial with a power $p$ of 3 as objective functions.

The AMS contains several muscle models. I included the simple muscle model and the three-element Hill-type muscle model. The simple muscle model does not consider the effect of muscle length and contract velocity on muscle strength. Instead, this model determines muscle strength as a proportional to the cross-sectional area of a muscle. The three-element Hill-type muscle model, based on the concept from Zajac (1989), contains the active element (active muscle fiber force), parallel passive element (passive muscle fiber elasticity), and serial passive

element of a muscle (passive tendon elasticity). Many factors are considered, such as the passive elasticity of muscle fibers and tendons and the pennation angle of muscle fibers. Therefore, the Hill-type muscle model has a nonlinear force-length and force-velocity relationship. Some factors, such as tendon and muscle fiber lengths, require calibration to match the anthropometry of each participant and fit the range of motion of the skeleton system during tasks. These factors were adjusted through a built-in calibration protocol in AMS. Other factors included in the Hill-type muscle model were defined within AMS.

### 2.5 Data Post-processing

In AMS, one muscle is usually represented by multiple muscle fibers, and each muscle fiber may have different muscle activity. Therefore, selecting appropriate muscle fibers is important for comparing muscle activity. I did so in three stages. First, I located the EMG electrodes in AMS based on anatomical landmarks using the same approach as when electrodes were placed on participants during data collection. Second, I selected the muscle fibers of the measured muscle that are directly covered by the electrodes. Third, I calculated the mean model-estimated muscle activity across the selected muscle fibers.

My analysis included a subset of the muscles monitored in the experiment. I included the muscle activity of the deltoid (anterior, middle, and posterior portions), upper trapezius, serratus anterior, and infraspinatus within the scope of my thesis, based on several reasons. First, according to Van Engelhoven et al. (2018b), the shoulderX substantially reduces upper trapezius, anterior deltoid, and infraspinatus muscle activity during an overhead drill task, so I included those muscles to test whether the human-exoskeleton model I used showed similar results. Second, the different task conditions in the study were likely to affect shoulder muscle activities,

and the shoulder muscles affected by these task conditions include those listed earlier. Including these muscles is crucial to test the ability of our human-exoskeleton models to predict shoulder muscle activity under various task conditions. Third, the infraspinatus, serratus anterior, and deltoid muscles are important shoulder stabilizers (Lee & An, 2002; Lugo et al., 2008). Aurbach et al. (2020) showed that infraspinatus and posterior deltoid muscle activity prediction was inaccurate during shoulder abduction. Therefore, I included these stabilizers to test our models in terms of predicting stabilizer activities.

## 2.6 Assessment Metrics

I used measures of pattern similarity and magnitude difference as assessment metrics to evaluate the model predictions. Pattern similarity between model-estimated muscle activity and normalized EMG (NEMG) was quantified using the maximum normalized cross-correlation (MNCC) in MATLAB (The MathWorks Inc., Natick, MA). This method evaluates the similarity in shape between two time series while disregarding uniform amplitude scaling. MNCC is derived from the normalized cross-correlation (NCC), defined as:

$$NCC(\tau) = \frac{\sum x_i y_{(i+\tau)}}{\sqrt{\sum x_i^2 \cdot \sum y_{(i+\tau)}^2}}$$

where $x_i$ and $y_i$ are two time series (here muscle activity and NEMG), and $i = 0, 1, 2, \ldots, N-1$. This approach outputs scalar values between 0 and 1, along with the time lag $\tau$ at which these values occur. MNCC determined the maximum scalar value and the corresponding time lag. To assess magnitude differences, I calculated the root mean square error (RMSE) between predicted muscle activity and NEMG expressed as a percentage of maximum muscle strength.

## 2.7 Statistical Analysis

I used separate three-way, repeated measures analyses of variance to assess the effects of ASE use (*Device*), task height (*Height*), and exertion direction (*Direction*) on pattern similarities and magnitude differences for each muscle of interest (i.e., AD, MD, PD, UT, SA, and IS). All analyses were done using JMP Pro 18 (SAS, Cary, NC) with the restricted maximum likelihood (REML) method. Significant main and interactive effects were explored using Tukey's HSD and simple effects tests, respectively. Statistical significance was concluded when $p < 0.05$. I also calculated effect size ($\eta^2$) for all main and interaction effects. According to Myors et al. (2010), I considered $\eta^2$ values of 0.01, 0.06, and 0.14 as small, medium, and large effect sizes, respectively.

My analysis had five independent variables: *Objective Function*, *Muscle Model*, *Device*, *Height*, and *Direction*. However, for simplicity only one combination of *Objective Function* and *Muscle Model* was selected, specifically minmax and the Hill-type muscle model; doing so allowed me to focus on analyzing the effects of *Device*, *Height*, and *Direction*. This combination was selected for two reasons. First, the Hill-type muscle model is more physiologically realistic than the simple muscle model. Preliminary results also showed that the Hill-type muscle model produced better pattern similarities than the simple muscle model. However, the Hill-type muscle model resulted in higher magnitude difference values. Second, there were *Objective Function* × *Muscle Model* interaction effects on pattern similarity for the AD and UT muscles. The minmax and Hill-type combination had the highest pattern similarity values for the AD and UT. There was no main effect of *Objective Function* on magnitude differences.

## 3. Results

ANOVA results ($p$ values) with effect size ($\eta^2$) are summarized in Tables 1 and 2 in the Appendix. For efficiency, the subsequent presentation of results will exclude effects that are significant but that had relatively small effect sizes ($\eta^2 < 0.01$).

### 3.1 Pattern Similarities

There were significant *Device* × *Height* × *Direction* interaction effects on pattern similarity for the AD, UT, and SA, with summary results provided in Figure 4. For the AD, model-estimated activity had pattern similarities > 0.7 without an ASE. When an ASE was used, these pattern similarities were reduced. In the upward *Direction*, SX resulted in significantly lower pattern similarities. The difference was 0.184 (21% reduction) at the medium *Height*, and this difference increased to 0.283 (38% reduction) at the high *Height*. In the forward Direction, the SX significantly reduced MNCC values at all *Heights* compared to ND, with respective decreases of 0.167 (23%), 0.184 (25%), and 0.203 (29%) at low, medium, and high *Heights*. For the AD overall, ASE use decreased pattern similarities in both the upward and forward *Directions*. The magnitude of this reduction increased with task height, especially when force was generated in the upward *Direction*.

Results similar to the AD were also found for the UT and SA muscles. Across most task conditions, model-estimated UT and SA muscle activity had high MNCC values (> 0.7). For the UT, using SX resulted in significantly lower MNCCs compared to ND at the combination of high *Height* and upward *Direction*. The reduction with SX use was 0.076 (9%). In the forward *Direction*, SX use resulted in lower MNCC values than ND across all *Heights*. However, the magnitude of these differences was small, with decreases of 0.046 (6%), 0.035 (5%), and 0.036

(5%) at the low, medium, and high *Heights*, respectively. For the SA muscle, SX use resulted in a significantly lower MNCC value in the upward *Direction*, with decreases of 0.066 (7%) at the medium *Height* and 0.135 (16%) at the high *Height*. In the forward *Direction*, SX resulted in significantly lower MNCC values, with decreases of 0.038 (5%) at the medium *Height* and 0.036 (5%) at the high *Height*. Again, similar to the AD, ASE use resulted in a greater reduction of MNCC values at higher *Heights* in the upward *Direction* for both the UT and SA, although the magnitudes of reduction were smaller than those for the AD. In the forward *Direction*, the magnitude of reduction resulting from ASE use was smaller than that observed for the AD, and the magnitude of this reduction was similar across *Heights*.

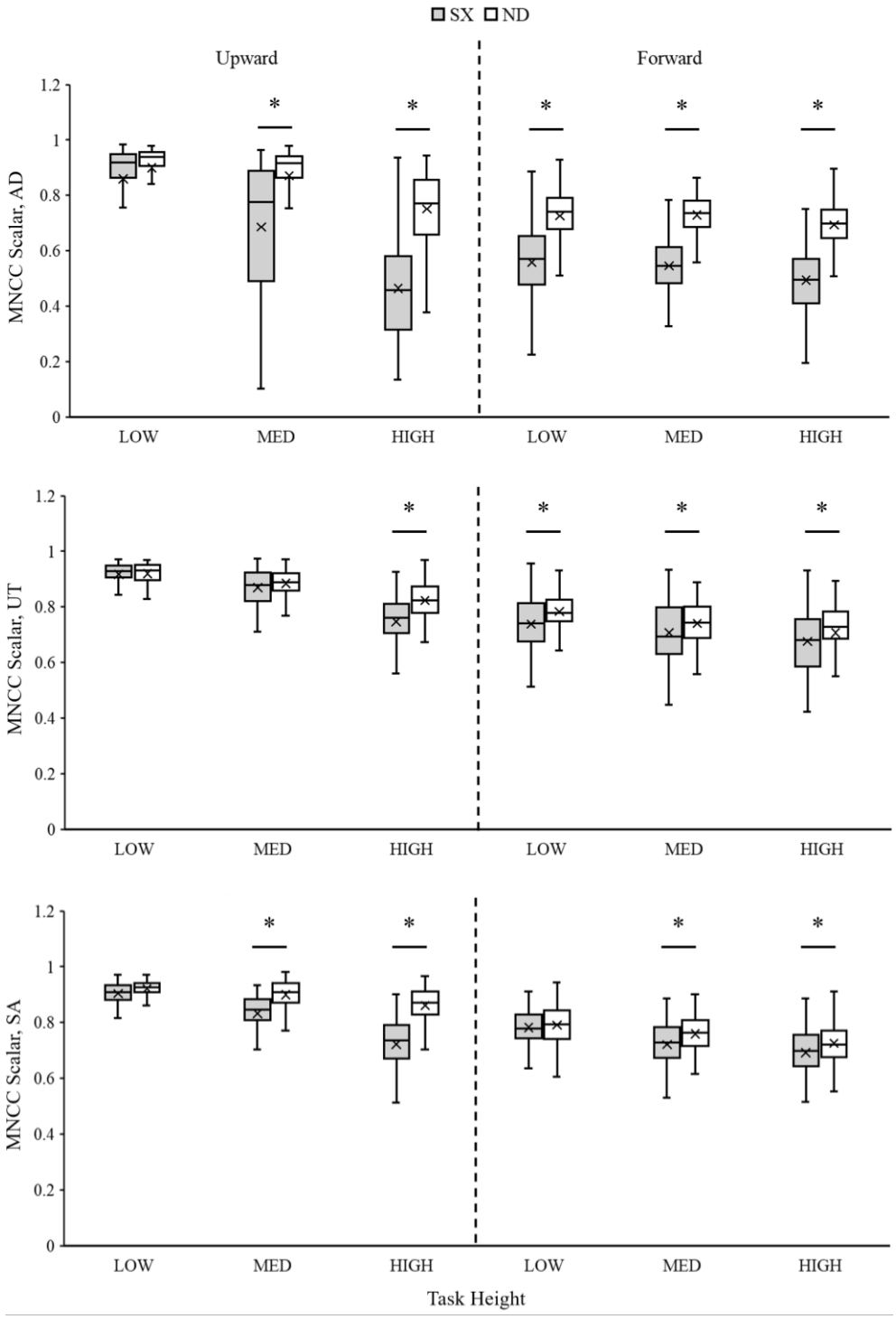


Figure 4. Box plots showing AD (top), UT (middle), and SA (bottom) pattern similarities (MNCC) with respect to *Device*, *Height*, and *Direction*. The symbol * denotes significant paired differences between using the SX exoskeleton and the control condition (ND).

*Height* × *Direction* interaction effects were significant for MD, PD, and IS pattern similarities (Figure 5). For the MD, MNCC values in the upward *Direction* were > 0.9 at the low and medium *Heights*, whereas MNCC values in the forward *Direction* were all below 0.7. MNCC values for both *Directions* decreased as *Height* increased, with the upward *Direction* resulting in a more substantial decrease. When comparing the differences between *Directions*, MNCC values in the forward *Direction* were significantly lower at all three *Heights*. These differences were 0.371 (34%), 0.288 (32%), and 0.190 (25%) at the low, medium, and high *Heights*, respectively.

Results for the IS were similar to those for the MD, in that the forward *Direction* resulted in significantly lower MNCC values at all *Heights*, and this difference decreased as *Height* increased. At the low *Height*, exertions in the forward *Direction* resulted in significantly lower MNCC values than in the upward *Direction*, with a difference of 0.131 (14%). This difference was reduced to 0.110 (12%) at the medium *Height* and 0.023 (3%) at the high *Height*.

Distinct results were observed for the PD compared with the MD and IS, in that MNCC values for the PD were lower than across all *Heights*. For the MD and IS, RMSE values in the upward *Direction* decreased more substantial as *Height* increased, whereas in the forward *Direction*, the RMSE values remained more stable across all *Heights*. For the PD, however, MNCC values decreased with increasing *Height* in both *Directions*, from ~0.7 at the low *Height* to ~0.4 at the high *Height*. Additionally, the variance in MNCC values for the PD was larger than that for the MD and IS.

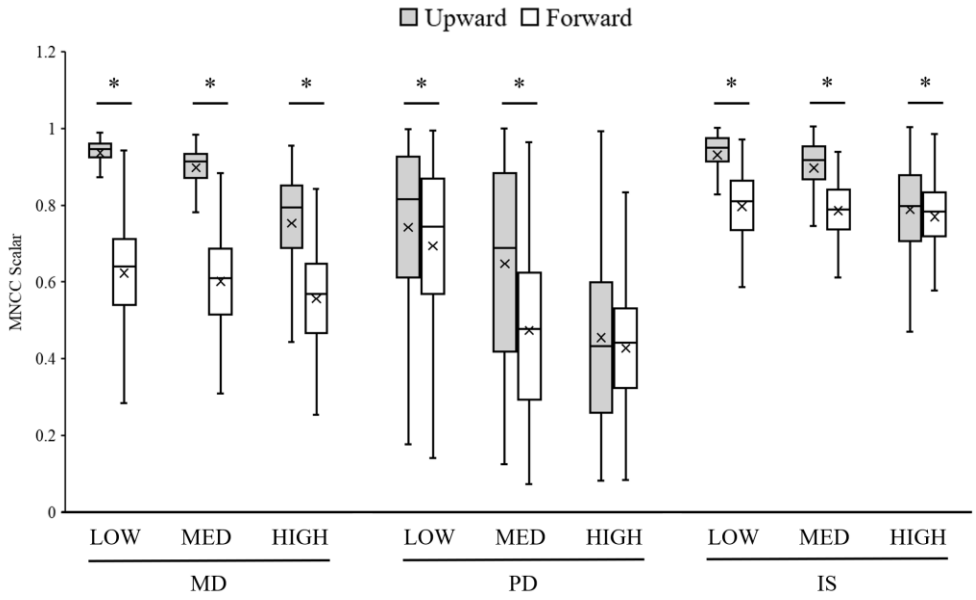


Figure 5. Box plots showing MD, PD, and IS pattern similarities (MNCC) with respect to *Height* and *Direction*. The symbol * denotes significant paired differences between the upward and forward push directions.

*Device* × *Height* interaction effects also significantly affected MD and PD pattern similarities (Figure 6). For the MD, SX resulted in significantly lower MNCC values at all *Heights*, and these differences increased as task *Height* increased, from 0.072 (9%) at the low Height to 0.095 (12%) at the medium *Height* and 0.133 (18%) at the high *Height*. For the PD, although SX also resulted in significantly lower MNCC values than ND, the pattern was different: the differences increased from 0.232 (28%) at the low *Height* to 0.311 (44%) at medium *Height*, then decreased to 0.222 (41%) at the high *Height*. This pattern for the PD contrasts with the monotonic increase observed for the MD with increasing *Height*.

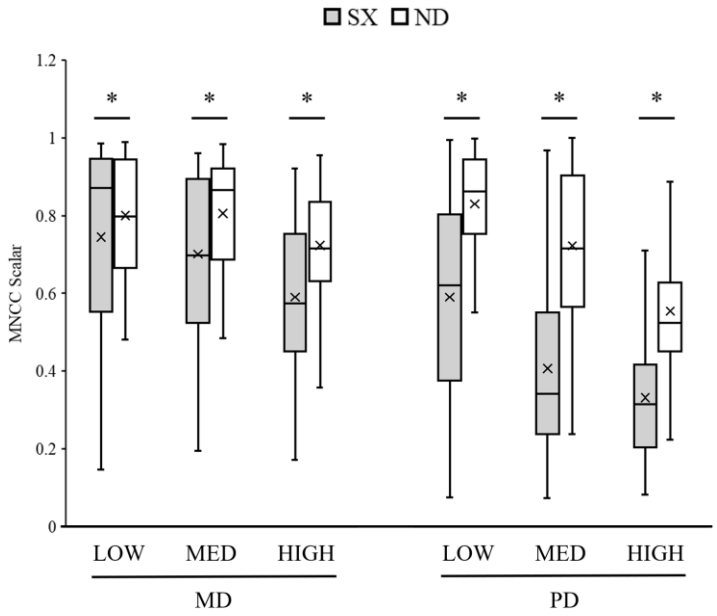


Figure 6. Box plots showing MD and PD pattern similarities (MNCC) with respect to *Device* and *Height*. The symbol * denotes significant paired differences between using the SX exoskeleton and the control condition (ND).

*Device* × *Direction* interaction effects significantly affected MD and IS pattern similarities (Figure 7). MNCC values were higher in the upward *Direction* for both the MD and IS. For the MD, SX resulted in lower MNCC values compared to ND in both the upward and forward *Directions*. In contrast, for the IS using the SX resulted in significantly higher MNCC values than ND in the forward *Direction*.

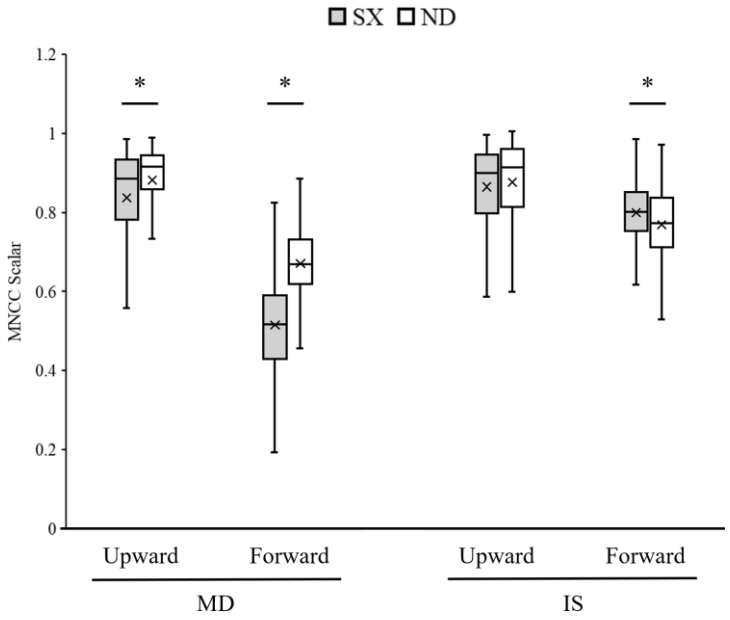


Figure 7. Box plots showing MD and IS pattern similarities (MNCC) with respect to *Device* and *Direction*. The symbol * denotes significant paired differences between using the SX exoskeleton and the control condition (ND).

3.2 Magnitude Differences

There were significant *Device* × *Height* × *Direction* interaction effects on magnitude differences for the AD, MD, and IS muscles (Figure 8). For the AD and MD muscles, ND resulted in significantly higher RMSE values at the high *Height* in the upward *Direction* compared to SX. The specific differences between ND and SX were 27.94 (79% increase) for the AD and 23.26 (37% increase) for the MD. In the upward *Direction*, RMSE values for the AD and MD significantly increased with *Height* for both *Devices*. Distinct results were obtained for the IS, for which significant differences between the two *Devices* were found in the upward *Direction* at the medium *Height* and the forward *Direction* at the high *Height*, with SX resulting in higher RMSE values in these conditions. RMSE values also increased with *Height* for the ISE in both the upward and forward *Directions*.

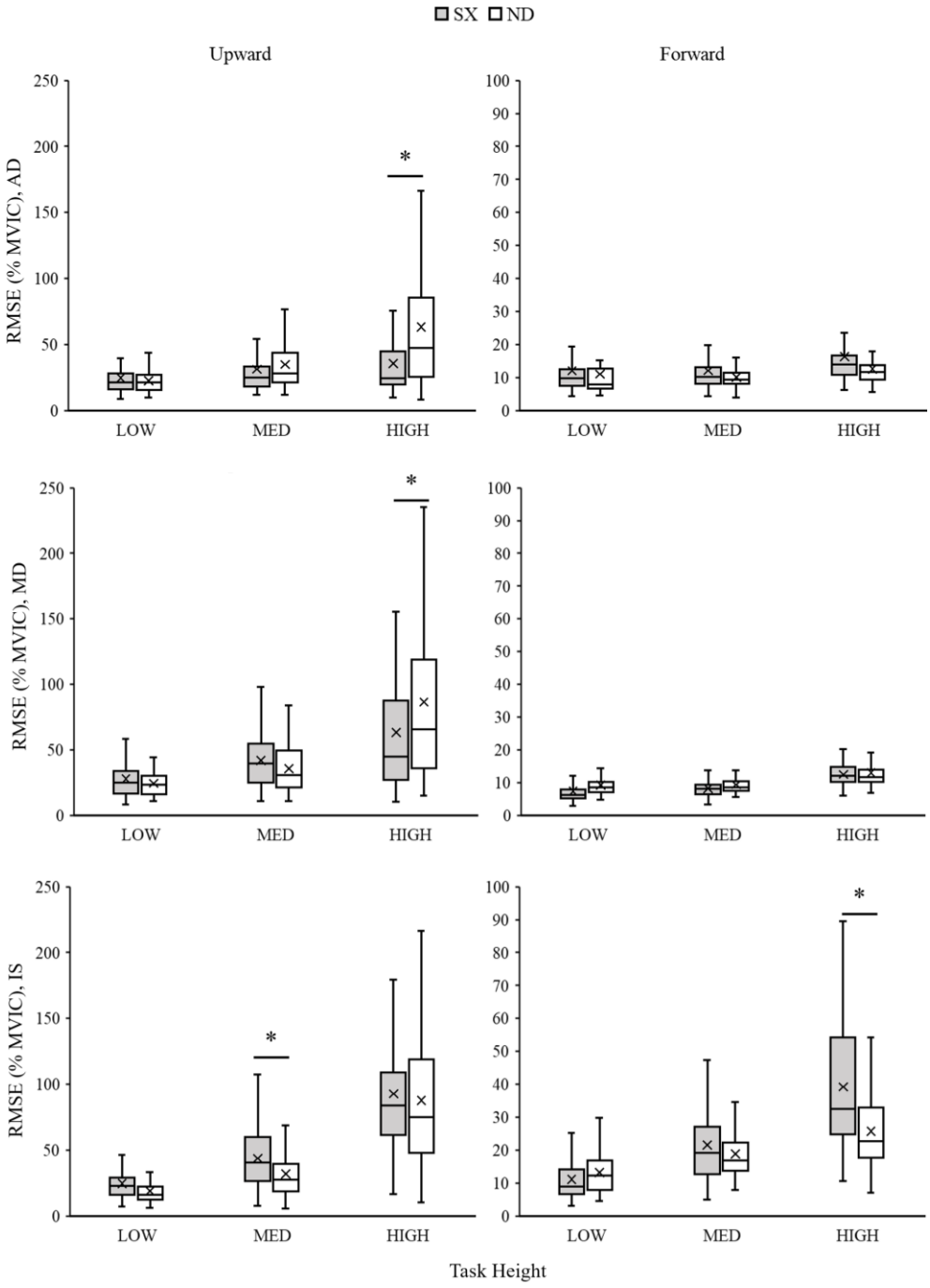


Figure 8. Box plots showing AD (top), MD (middle), and IS (bottom) magnitude difference (RMSE) with respect to *Device*, *Height*, and *Direction*. The symbol * denotes significant paired differences between using the SX exoskeleton and the control condition (ND).

*Device* × *Height* interaction effects significantly affected UT, PD, and SA magnitude differences (Figure 9). For the UT and SA muscles, ND resulted in significantly higher magnitude

differences than SX at the high *Height*. RMSE values increased with *Height* for both the UT and SA. For the PD muscle, ND resulted in higher magnitude differences compared to SX at the low and medium *Heights*.

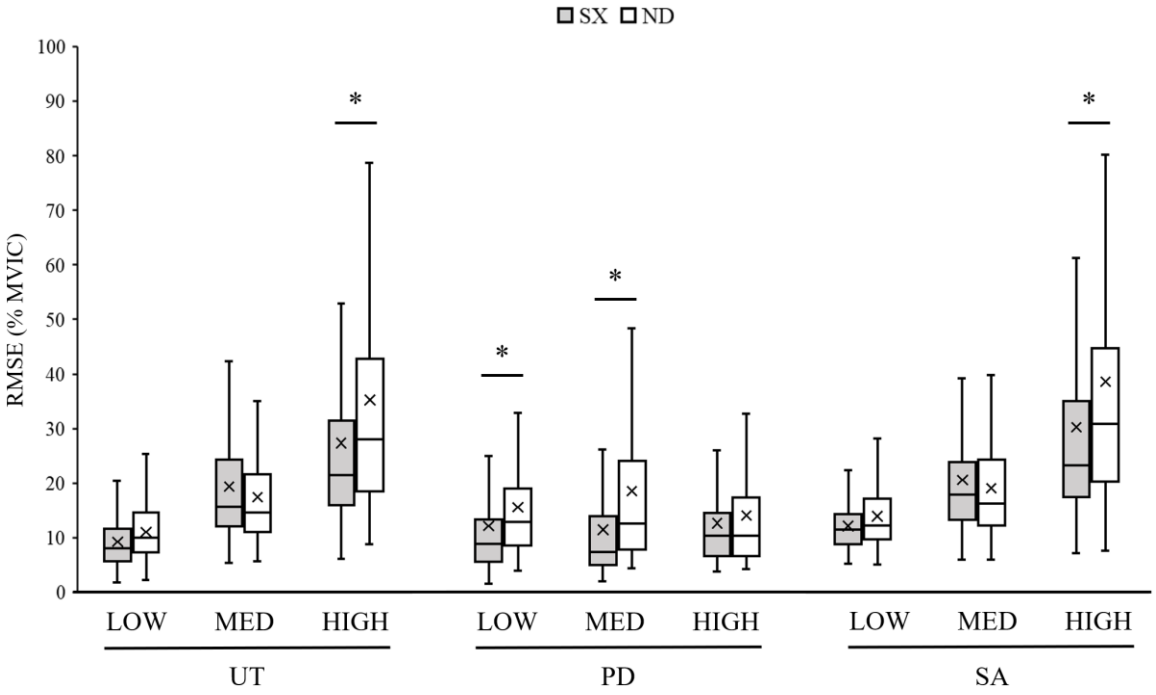


Figure 9. Box plots showing UT, PD, and SA magnitude difference (RMSE) with respect to *Device* and *Height*. The symbol * denotes significant paired differences between using the SX exoskeleton and the control condition (ND).

There was a significant *Direction* × *Height* interaction effect on magnitude differences for the UT muscle (Figure 10). The upward *Direction* resulted in a significantly larger RMSE value at the medium *Height* compared to the forward Direction. Finally, there was a significant *Device* × *Direction* interaction effect on magnitude differences for the PD muscle (Figure 11). SX resulted in a significantly higher RMSE value in the upward *Direction* compared to ND.

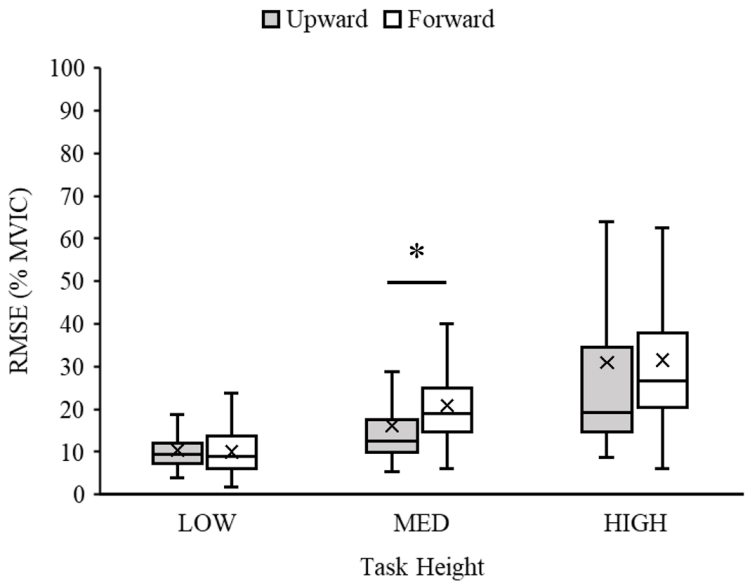


Figure 10. Box plots showing UT magnitude difference (RMSE) with respect to *Height* and *Direction*. The symbol * denotes significant paired differences between the upward and forward push directions.

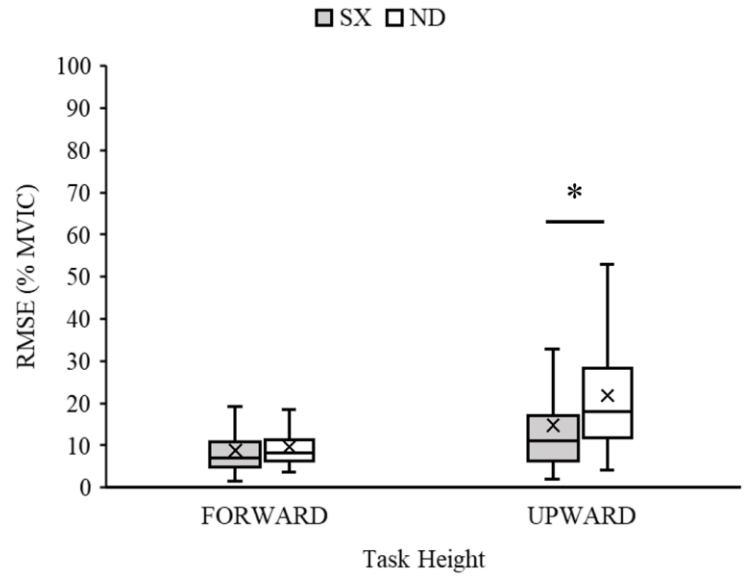


Figure 11. Box plots showing PD magnitude difference (RMSE) with respect to *Device* and *Direction*. The symbol * denotes significant paired differences between using the SX exoskeleton and the control condition (ND).

## 4. Discussion

I evaluated whether including an ASE affects model-estimated shoulder muscle activity and whether task conditions influence such estimations. Although results from previous studies

indicate that musculoskeletal models can estimate shoulder muscle activity with reasonable accuracy at lower arm elevation angles, these studies either involved relatively simple tasks (Aurbach et al., 2020; Nikooyan et al., 2011) or included a limited number of muscle groups (Fritzsche et al., 2021). Moreover, no existing evidence indicates whether the performance of musculoskeletal models is affected by ASE use. Therefore, I evaluated estimates of the activity in six muscle groups, obtained from a commercial biomechanical model. These evaluations were done using NEMG obtained in a previous investigation during dynamic overhead push tasks with and without an ASE.

Musculoskeletal models of the shoulder typical provide reasonable estimates of shoulder muscle activity during neutral tasks involve limited arm elevation. Nikooyan et al. (2010), for example, reported high correlations between model-estimated GH-JRF and *in vivo* measurements ($R > 0.96$) during arm abduction and flexion at arm elevation angles < 90°. Nikooyan et al. (2011) also showed a good correlation between model-estimated muscle force and NEMG ($R > 0.8$) for the AD. Similar to findings in these previous studies, my results showed good agreement between model-estimated shoulder muscle activity and NEMG at the low *Height* in the upward *Direction*. Pattern similarity values were close to or above 0.9 across most muscle groups, both with and without an ASE. The specific differences between model estimations and NEMG in this particular task condition ranged from 10 to 25% MVIC. By demonstrating excellent pattern similarity and moderate magnitude differences relative to NEMG, these findings supported my first hypothesis that model-estimated shoulder muscle activity would correlate well with NEMG at lower task *Heights*. These findings also extend previous evidence by showing that musculoskeletal models not only perform well under simple task conditions but also estimate

shoulder muscle activity with reasonable accuracy under specific dynamic overhead tasks with ASE use.

Results from previous studies indicate that the performance of shoulder musculoskeletal models is reduced with increasing arm elevation angle (Aurbach et al., 2020; Nikooyan et al., 2010; Nikooyan et al., 2011). This reduction may results because larger arm elevation angles typically require a more complex pattern of shoulder muscle activation (Chopp et al., 2010). My results agreed with these findings, since MNCC values decreased as *Height* increased (Figures 4-6), and magnitude difference increased as *Height* increased (Figures 8-10), although not all such differences were significant. My results also add to findings from previous studies that including an ASE resulted in lower pattern similarities, especially at higher arm elevation angles (Figures 4 and 6). These findings from this study partially support my second hypothesis that ASE use would adversely affect both pattern similarity and magnitude difference metrics. Although ASE use reduced pattern similarity values, magnitude differences were also reduced (Figures 8, 9, and 11).

I suggest several possible explanations for the finding that ASE use reduced pattern similarities, especially with elevated arm postures. First, the kinematics data I used was captured by an MMC system. Although these systems appear to be reliable (Khoshelham & Elberink, 2012; Nakaizumi et al., 2024; Tölgyessy et al., 2021), the process of extracting BVH files may have introduced errors in estimated joint angles due to soft-tissue artifacts and clothing (Antico et al., 2021), and including an ASE could have exaggerate these errors. In AMS, shoulder girdle movement was determined by the arm elevation angle, therefore any error in shoulder elevation angle could

translate to additional errors in shoulder kinematics in AMS and ultimately affect estimated shoulder muscle activity.

Second, SuitX provided the torque profile for the ShoulderX as a function of arm elevation angle. In AMS, this torque was applied to the joint connecting the arm frame and shoulder frame (see Figure 2), making it a function of the ASE joint angle. Although ShoulderX was designed to follow the upper arm, the arm frame could slide along the long axis of the upper arm, causing discrepancies between the ASE joint and actual arm elevation angles. Since the ASE joint angle was used to calculate the supportive torque, it was adjusted to match the arm elevation angle. This approach, though, could have introduced errors in the simulated support torque, thereby affecting the model-estimated muscle activity. Third, the support torque in AMS was transferred to the upper arm through contact forces applied at a fixed point along the humerus, with the location of this point determined by the shoulderX arm frame length. However, the arm frame could slide and rotate along the upper arm during an overhead push, causing the actual contact point to shift. This shift in the contact point could lead to errors in the model-estimated shoulder muscle activity.

ASE use reduced RMSE values (i.e., the magnitude differences between model-predictive activity and NEMG) for the AD, MD, PD, UT, and SA but increased RMSE values for the IS. Notably, some RMSE values exceeded 100 %MVIC, primarily in the high *Height* and upward *Direction* condition (Figure 8). These muscle overload instances occurred randomly across participants of varying height, body mass, and biological sex, with no specific anthropometric group exhibiting more such instances than others. These larger RMSE values are likely due to muscle overload in the model-based simulation, in which the force required to perform a motion

exceeded the maximum muscle strength. In these cases, model-estimated muscle activity surpassed 100% MVIC while NEMG remained within normal limits, leading to One possible reason for muscle overload is that the Hill-type muscle model includes both active and passive elements, with passive stiffness activating when muscle fibers stretch beyond a threshold (Aurbach et al., 2020). During overhead tasks, especially at elevated arm posture, antagonist muscles (e.g., latissimus dorsi) can become stretched, forcing agonist muscles (e.g., AD) to exert extra force to counterbalance passive stiffness from antagonist muscles. In the upward push *Direction*, the agonist muscles must generate enough force to push the target while overcoming this passive resistance, which can lead to muscle overload. Under these conditions, simulated shoulder muscle activity largely exceeded NEMG levels. Applying ASE support torque reduced the force required by agonist muscles, resulting in lower estimated activity for most muscle groups. In contrast, because the IS contracts opposite to the support torque direction, the estimated IS activity increased with ASE use, leading to higher RMSE values. Muscle overload could also indicate that the performance of musculoskeletal models reduces at extreme arm postures.

This work has several limitations that should be considered in addition to those noted earlier. First, the MMC system is critical to the accuracy of model-estimated shoulder muscle activity. Unlike marker-based motion capture, MMC systems are less accurate and may introduce joint angle errors into AMS (Antico et al., 2021). Capturing separate motions of the ASE and human body segments using the MMC system is not a straightforward process. Therefore, I assumed that the ASE kinematics followed those of the upper arm. Any discrepancy between these kinematics could introduce errors to the model-estimated muscle activity. Future studies could use marker-based motion capture to monitor both human and ASE motions, which may yield

more accurate estimation of ASE support torque and contact force locations. Second, the muscle strength scaling in AMS was based on anthropometric data instead of direct measurements, and this scaling process used a generic model that does not consider sex-based differences. Future work could examine how biological sex influences model-estimated shoulder muscle activity and incorporate sex-specific models to improve accuracy. Third, model-estimated muscle activity was extracted by averaging the activity of muscle fibers directly beneath the EMG electrodes, which might not fully represent the muscle fibers contributing to the EMG signal. In reality, muscle crosstalk (Barbero et al., 2012) or muscle belly shift (Rajaratnam, 2014; Solomonow et al., 1994) could also affect EMG signals. Fourth, I only included one ASE, and the generalizability of my results to other ASE devices is unknown. Future studies should include multiple ASE devices to determine whether the results extend across different ASEs.

In summary, this thesis was motivated by the need to simplify the exoskeleton evaluation process by replacing some EMG measurements with model-estimated muscle activity. No prior evidence has indicated whether ASE use affects shoulder muscle activity or how such effects vary with task conditions. Therefore, I compared model-estimated shoulder muscle activity with NEMG under diverse task conditions, both with and without ASE use. I used pattern similarity and magnitude differences as evaluation metrics. My results indicate that ASE use generally reduces model performance, with the extent of this effect depending on the task. Model estimations were reasonably accurate under the low *Height* and upward *Direction* task condition, suggesting that model predictions can potentially replace EMG in similar task settings. However, the generalizability of these findings to other ASE devices remains uncertain. My results indicate that model performance declines at more extreme arm elevation angles and that ASE use

exacerbates this decline, underscoring the need to improve model performance when simulating extreme arm postures.

5. Bibliography


Albers, J. T., & Estill, C. F. (2007). *Simple solutions: Ergonomics for construction workers*. US Department of Health and Human Services, Public Health Service, Centers ….

Alwasel, A., Elrayes, K., Abdel-Rahman, E. M., & Haas, C. (2011). Sensing construction work-related musculoskeletal disorders (WMSDs). *ISARC Proc*, 164-169.

Antico, M., Balletti, N., Laudato, G., Lazich, A., Notarantonio, M., Oliveto, R., Ricciardi, S., Scalabrino, S., & Simeone, J. (2021). Postural control assessment via Microsoft Azure Kinect DK: An evaluation study. *Computer Methods and Programs in Biomedicine*, *209*, 106324.

Auer, S., Tröster, M., Schiebl, J., Iversen, K., Chander, D. S., Damsgaard, M., & Dendorfer, S. (2022). Biomechanical assessment of the design and efficiency of occupational exoskeletons with the AnyBody Modeling System. *Zeitschrift für Arbeitswissenschaft*, *76*(4), 440-449. https://doi.org/10.1007/s41449-022-00336-4

Aurbach, M., Spicka, J., Suss, F., & Dendorfer, S. (2020). Evaluation of musculoskeletal modelling parameters of the shoulder complex during humeral abduction above 90 degrees. *J Biomech*, *106*, 109817. https://doi.org/10.1016/j.jbiomech.2020.109817

Barbero, M., Merletti, R., & Rainoldi, A. (2012). *Atlas of muscle innervation zones: understanding surface electromyography and its applications*. Springer Science & Business Media.

Bernard, B. P., & Putz-Anderson, V. (1997). Musculoskeletal disorders and workplace factors; a critical review of epidemiologic evidence for work-related musculoskeletal disorders of the neck, upper extremity, and low back. https://stacks.cdc.gov/view/cdc/21745

Blanco, A., Catalán, J. M., Díez, J. A., García, J. V., Lobato, E., & García-Aracil, N. (2019). Electromyography Assessment of the Assistance Provided by an Upper-Limb Exoskeleton in Maintenance Tasks. *Sensors*, *19*(15), 3391. https://doi.org/10.3390/s19153391

Chopp, J. N., Fischer, S. L., & Dickerson, C. R. (2010). The impact of work configuration, target angle and hand force direction on upper extremity muscle activity during sub-maximal overhead work. *Ergonomics*, *53*(1), 83-91.

Crowninshield, R. D., & Brand, R. A. (1981). A physiologically based criterion of muscle force prediction in locomotion. *Journal of Biomechanics*, *14*(11), 793-801.

De Bock, S., Ghillebert, J., Govaerts, R., Elprama, S. A., Marusic, U., Serrien, B., Jacobs, A., Geeroms, J., Meeusen, R., & De Pauw, K. (2021). Passive Shoulder Exoskeletons: More Effective in the Lab Than in the Field? *IEEE Trans Neural Syst Rehabil Eng*, *29*, 173-183. https://doi.org/10.1109/TNSRE.2020.3041906

de Kok, J., Vroonhof, P., Snijders, J., Roullis, G., Clarke, M., Peereboom, K., Dorst, P. v., & Isusi, I. (2019). *Work-related musculoskeletal disorders: prevalence, costs and demographics in the EU*.

de Looze, M. P., Bosch, T., Krause, F., Stadler, K. S., & O'Sullivan, L. W. (2016). Exoskeletons for industrial application and their potential effects on physical work load. *Ergonomics*, *59*(5), 671-681. https://doi.org/10.1080/00140139.2015.1081988

Desbrosses, K., Schwartz, M., & Theurel, J. (2021). Evaluation of two upper-limb exoskeletons during overhead work: influence of exoskeleton design and load on muscular adaptations and balance regulation. *Eur J Appl Physiol*, *121*(10), 2811-2823. https://doi.org/10.1007/s00421-021-04747-9

Fritzsche, L., Galibarov, P. E., Gärtner, C., Bornmann, J., Damsgaard, M., Wall, R., Schirrmeister, B., Gonzalez-Vargas, J., Pucci, D., Maurice, P., Ivaldi, S., & Babič, J. (2021). Assessing the efficiency of exoskeletons in physical strain reduction by biomechanical simulation with AnyBody Modeling System. *Wearable Technologies*, *2*. https://doi.org/10.1017/wtc.2021.5

Gillette, J. C., & Stephenson, M. L. (2019). Electromyographic Assessment of a Shoulder Support Exoskeleton During on-Site Job Tasks. *IISE Transactions on Occupational Ergonomics and Human Factors*, *7*(3-4), 302-310. https://doi.org/10.1080/24725838.2019.1665596

Gneiting, E., Schiebl, J., Tröster, M., Kopp, V., Maufroy, C., & Schneider, U. (2022). Model-Based Biomechanics for Conceptual Exoskeleton Support Estimation Applied for a Lifting Task. In (pp. 395-399). Springer International Publishing. https://doi.org/10.1007/978-3-030-69547-7_64

Grazi, L., Trigili, E., Proface, G., Giovacchini, F., Crea, S., & Vitiello, N. (2020). Design and Experimental Evaluation of a Semi-Passive Upper-Limb Exoskeleton for Workers With Motorized Tuning of Assistance. *IEEE Trans Neural Syst Rehabil Eng*, *28*(10), 2276-2285. https://doi.org/10.1109/TNSRE.2020.3014408

Khoshelham, K., & Elberink, S. O. (2012). Accuracy and Resolution of Kinect Depth Data for Indoor Mapping Applications. *Sensors*, *12*(2), 1437-1454. https://doi.org/10.3390/s120201437

Kim, S., Nussbaum, M. A., Mokhlespour Esfahani, M. I., Alemi, M. M., Alabdulkarim, S., & Rashedi, E. (2018). Assessing the influence of a passive, upper extremity exoskeletal vest for tasks requiring arm elevation: Part I - "Expected" effects on discomfort, shoulder muscle activity, and work task performance. *Appl Ergon*, *70*, 315-322. https://doi.org/10.1016/j.apergo.2018.02.025

Kim, S., Nussbaum, M. A., Smets, M., & Ranganathan, S. (2021). Effects of an arm-support exoskeleton on perceived work intensity and musculoskeletal discomfort: An 18-month field study in automotive assembly. *Am J Ind Med*, *64*(11), 905-914. https://doi.org/10.1002/ajim.23282

Kong, Y. K., Choi, K. H., Cho, M. U., Kim, S. Y., Kim, M. J., Shim, J. W., Park, S. S., Kim, K. R., Seo, M. T., Chae, H. S., & Shim, H. H. (2022). Ergonomic Assessment of a Lower-Limb Exoskeleton through Electromyography and Anybody Modeling System. *Int J Environ Res Public Health*, *19*(13). https://doi.org/10.3390/ijerph19138088

Lee, S.-B., & An, K.-N. (2002). Dynamic glenohumeral stability provided by three heads of the deltoid muscle. *Clinical Orthopaedics and Related Research®*, *400*, 40-47.

Lowe, B. D., Billotte, W. G., & Peterson, D. R. (2019). ASTM F48 Formation and Standards for Industrial Exoskeletons and Exosuits. *IISE Trans Occup Ergon Hum Factors*, *7*. https://doi.org/10.1080/24725838.2019.1579769

Lugo, R., Kung, P., & Ma, C. B. (2008). Shoulder biomechanics. *European journal of radiology*, *68*(1), 16-24.

Madinei, S., & Nussbaum, M. A. (2023). Estimating lumbar spine loading when using back-support exoskeletons in lifting tasks. *J Biomech*, *147*, 111439. https://doi.org/10.1016/j.jbiomech.2023.111439

Michaud, F., Lamas, M., Lugrís, U., & Cuadrado, J. (2021). A fair and EMG-validated comparison of recruitment criteria, musculotendon models and muscle coordination

strategies, for the inverse-dynamics based optimization of muscle forces during gait. *Journal of NeuroEngineering and Rehabilitation*, *18*, 1-15.
Myors, B., Murphy, K. R., & Wolach, A. (2010). *Statistical power analysis: A simple and general model for traditional and modern hypothesis tests*. Routledge.
Nakaizumi, D., Nishimura, T., Inaoka, P. T., & Asai, H. (2024). Reliability and validity of a method to measure trunk rotation angle from images using a camera and posture mirror. *Medical Engineering & Physics*, *131*, 104224.
Nikooyan, A. A., Veeger, H. E., Westerhoff, P., Graichen, F., Bergmann, G., & van der Helm, F. C. (2010). Validation of the Delft Shoulder and Elbow Model using in-vivo glenohumeral joint contact forces. *J Biomech*, *43*(15), 3007-3014. https://doi.org/10.1016/j.jbiomech.2010.06.015
Nikooyan, A. A., Veeger, H. E. J., Chadwick, E. K. J., Praagman, M., & Van Der Helm, F. C. T. (2011). Development of a comprehensive musculoskeletal model of the shoulder and elbow. *Medical & Biological Engineering & Computing*, *49*(12), 1425-1435. https://doi.org/10.1007/s11517-011-0839-7
Ojelade, A., Morris, W., Kim, S., Kelson, D., Srinivasan, D., Smets, M., & Nussbaum, M. A. (2023). Three passive arm-support exoskeletons have inconsistent effects on muscle activity, posture, and perceived exertion during diverse simulated pseudo-static overhead nutrunning tasks. *Appl Ergon*, *110*, 104015. https://doi.org/10.1016/j.apergo.2023.104015
Pacifico, I., Parri, A., Taglione, S., Sabatini, A. M., Violante, F. S., Molteni, F., Giovacchini, F., Vitiello, N., & Crea, S. (2022). Exoskeletons for workers: A case series study in an enclosures production line. *Appl Ergon*, *101*, 103679. https://doi.org/10.1016/j.apergo.2022.103679
Pinho, J. P., & Forner-Cordero, A. (2022). Shoulder muscle activity and perceived comfort of industry workers using a commercial upper limb exoskeleton for simulated tasks. *Appl Ergon*, *101*, 103718. https://doi.org/10.1016/j.apergo.2022.103718
Pinho, J. P., Parik Americano, P., Taira, C., Pereira, W., Caparroz, E., & Forner-Cordero, A. (2020, 2020). Shoulder muscles electromyographic responses in automotive workers wearing a commercial exoskeleton. IEEE,
Rajaratnam, B. (2014). CH Goh J, Kumar VP (2014) A Comparison of EMG Signals from Surface and Fine-Wire Electrodes During Shoulder Abduction. *Int J Phys Med Rehabil*, *2*(206), 2.
Rashedi, E., Kim, S., Nussbaum, M. A., & Agnew, M. J. (2014). Ergonomic evaluation of a wearable assistive device for overhead work. *Ergonomics*, *57*(12), 1864-1874. https://doi.org/10.1080/00140139.2014.952682
Rasmussen, J., Damsgaard, M., & Voigt, M. (2001). Muscle recruitment by the min/max criterion—a comparative numerical study. *Journal of Biomechanics*, *34*(3), 409-415.
Roquelaure, Y., Ha, C., Rouillon, C., Fouquet, N., Leclerc, A., Descatha, A., Touranchet, A., Goldberg, M., Imbernon, E., & Members of Occupational Health Services of the Pays de la Loire, R. (2009). Risk factors for upper-extremity musculoskeletal disorders in the working population. *Arthritis Rheum*, *61*(10), 1425-1434. https://doi.org/10.1002/art.24740
Schmalz, T., Colienne, A., Bywater, E., Fritzsche, L., Gartner, C., Bellmann, M., Reimer, S., & Ernst, M. (2022). A Passive Back-Support Exoskeleton for Manual Materials Handling: Reduction of Low Back Loading and Metabolic Effort during Repetitive Lifting. *IISE*

*Trans Occup Ergon Hum Factors*, *10*(1), 7-20. https://www.ncbi.nlm.nih.gov/pubmed/34763618

Seiferheld, B. E., Frost, J., Krog, M., Skals, S., & Andersen, M. S. (2022). Biomechanical investigation of a passive upper-extremity exoskeleton for manual material handling - a computational parameter study and modelling approach. *International journal of human factors modelling and simulation*, *7*(3/4), 275. https://doi.org/10.1504/ijhfms.2022.124304

Solomonow, M., Baratta, R., Bernardi, M., Zhou, B., Lu, Y., Zhu, M., & Acierno, S. (1994). Surface and wire EMG crosstalk in neighbouring muscles. *Journal of Electromyography and Kinesiology*, *4*(3), 131-142.

Sommerich, C. M., & Hughes, R. E. (2006). Aetiology of work-related disorders of the rotator cuff tendons: Research and theory. *Theoretical Issues in Ergonomics Science*, *7*(1), 19-38. https://doi.org/10.1080/14639220512331335133

Tölgyessy, M., Dekan, M., Chovanec, Ľ., & Hubinský, P. (2021). Evaluation of the azure kinect and its comparison to kinect v1 and kinect v2. *Sensors*, *21*(2), 413.

Troster, M., Wagner, D., Muller-Graf, F., Maufroy, C., Schneider, U., & Bauernhansl, T. (2020). Biomechanical Model-Based Development of an Active Occupational Upper-Limb Exoskeleton to Support Healthcare Workers in the Surgery Waiting Room. *Int J Environ Res Public Health*, *17*(14). https://doi.org/10.3390/ijerph17145140

U.S. Bureau of Labor Statistics. (2020). *Case circumstances and worker characteristics for injuries and illnesses involving days away from work - 2020, MSD by part of body affected by days away from work (Number, Rate, Median)*. U.S. Bureau of Labor Statistics. Retrieved 17 September from https://www.bls.gov/iif/nonfatal-injuries-and-illnesses-tables.htm#dafw

Van Der Helm, F. C. T. (1994). ANALYSIS OF THE KINEMATIC AND DYNAMIC BEHAVIOR OF THE SHOULDER MECHANISM. *Journal of Biomechanics*, *27*(5), 527-550.

Van der Molen, H. F., Foresti, C., Daams, J. G., Frings-Dresen, M. H., & Kuijer, P. P. F. (2017). Work-related risk factors for specific shoulder disorders: a systematic review and meta-analysis. *Occupational and environmental medicine*, *74*(10), 745-755.

Van Engelhoven, L., Poon, N., Kazerooni, H., Barr, A., Rempel, D., & Harris-Adamson, C. (2018a). Evaluation of an adjustable support shoulder exoskeleton on static and dynamic overhead tasks. *Proceedings of the Human Factors and Ergonomics Society Annual Meeting*, *62*(1), 804-808. https://doi.org/10.1177/1541931218621184

Van Engelhoven, L., Poon, N., Kazerooni, H., Barr, A., Rempel, D., & Harris-Adamson, C. (2018b). Evaluation of an adjustable support shoulder exoskeleton on static and dynamic overhead tasks. Proceedings of the Human Factors and Ergonomics Society Annual Meeting,

Wærsted, M., Koch, M., & Veiersted, K. B. (2020). Work above shoulder level and shoulder complaints: a systematic review. *International Archives of Occupational and Environmental Health*, *93*(8), 925-954. https://doi.org/10.1007/s00420-020-01551-4

Zajac, F. E. (1989). Muscle and tendon: properties, models, scaling, and application to biomechanics and motor control. *Critical reviews in biomedical engineering*, *17*(4), 359-411.

Zhou, X., & Zheng, L. (2021). Model-Based Comparison of Passive and Active Assistance Designs in an Occupational Upper Limb Exoskeleton for Overhead Lifting. *IISE Trans*

*Occup Ergon Hum Factors*, *9*(3-4), 167-185.
https://www.ncbi.nlm.nih.gov/pubmed/34254566

6. Appendix

Table 1: Summary of ANOVA results ($p$) with effect size ($\eta^2$) for **pattern similarities**. Significant effects ($p < 0.05$) and medium or larger effect sizes ($\eta^2 > 0.06$) are highlighted in bold font.

| Muscle Group | | Device (DE) | Height (H) | Direction (DR) | DE×H | DE×DR | H×DR | DE×H×DR |
|---|---|---|---|---|---|---|---|---|
| AD | $p$ | **<.0001** | **<.0001** | **<.0001** | **<.0001** | 0.2287 | **<.0001** | **<.0001** |
| | $\eta^2$ | **0.300** | **0.189** | **0.189** | 0.042 | 0.001 | **0.100** | 0.024 |
| MD | $p$ | **<.0001** | **<.0001** | **<.0001** | **<.0001** | **<.0001** | **<.0001** | 0.5878 |
| | $\eta^2$ | **0.218** | **0.227** | **0.664** | 0.018 | **0.084** | **0.076** | 0.001 |
| PD | $p$ | **<.0001** | **<.0001** | **<.0001** | **<.0001** | 0.3434 | **<.0001** | **0.0191** |
| | $\eta^2$ | **0.366** | **0.295** | 0.048 | 0.014 | 0.001 | 0.028 | 0.005 |
| UT | $p$ | **<.0001** | **<.0001** | **<.0001** | **0.0005** | 0.3715 | **<.0001** | **<.0001** |
| | $\eta^2$ | 0.052 | **0.231** | **0.439** | 0.009 | 0.000 | 0.040 | 0.013 |
| IS | $p$ | **0.0004** | **<.0001** | **<.0001** | **0.0005** | **<.0001** | **<.0001** | **0.0252** |
| | $\eta^2$ | 0.008 | **0.173** | **0.234** | 0.009 | 0.017 | **0.079** | 0.005 |
| SA | $p$ | **<.0001** | **<.0001** | **<.0001** | **<.0001** | **<.0001** | **<.0001** | **<.0001** |
| | $\eta^2$ | **0.135** | **0.251** | **0.417** | 0.043 | 0.029 | 0.020 | 0.022 |

Table 2: Summary of ANOVA results ($p$) with effect size ($\eta^2$) for **magnitude differences**. Significant effects ($p < 0.05$) and medium or larger effect sizes ($\eta^2 > 0.06$) are highlighted in bold font.

| Muscle Group | | Device (DE) | Height (H) | Direction (DR) | DE×H | DE×DR | H×DR | DE×H×DR |
|---|---|---|---|---|---|---|---|---|
| AD | $p$ | **<.0001** | **<.0001** | **<.0001** | **<.0001** | **<.0001** | **<.0001** | **<.0001** |
| | $\eta^2$ | 0.015 | **0.111** | **0.305** | 0.025 | 0.029 | **0.069** | 0.041 |
| MD | $p$ | **0.005** | **<.0001** | **<.0001** | **<.0001** | 0.1652 | **<.0001** | **<.0001** |
| | $\eta^2$ | 0.005 | **0.192** | **0.366** | 0.017 | 0.001 | **0.135** | 0.020 |
| PD | $p$ | **<.0001** | **0.0056** | **<.0001** | **<.0001** | **<.0001** | **0.0006** | 0.0694 |
| | $\eta^2$ | 0.040 | 0.006 | **0.166** | 0.013 | 0.022 | 0.009 | 0.003 |
| UT | $p$ | **<.0001** | **<.0001** | **0.0195** | **<.0001** | 0.0573 | **0.0001** | 0.2202 |
| | $\eta^2$ | 0.016 | **0.361** | 0.003 | 0.033 | 0.002 | 0.011 | 0.002 |
| IS | $p$ | **<.0001** | **<.0001** | **<.0001** | **0.0006** | 0.2235 | **<.0001** | **0.0001** |
| | $\eta^2$ | 0.020 | **0.471** | **0.338** | 0.009 | 0.001 | **0.224** | 0.011 |
| SA | $p$ | **<.0001** | **<.0001** | **<.0001** | **<.0001** | 0.2757 | **0.007** | 0.2679 |
| | $\eta^2$ | 0.017 | **0.327** | 0.016 | 0.028 | 0.001 | 0.006 | 0.002 |